Materials Research, Vol. 4, No. 4, 231-236, 2001.

Densification Studies of Silicon Carbide-Based Ceramics with Yttria, Silica and Alumina as Sintering Additives

J. Marchi, J.C. Bressiani, A.H.A. Bressiani

Instituto de Pesquisas Energéticas e Nucleares, Travessa R 400, Cidade Universitária, 05508-900 São Paulo - SP, Brasil

Received: November 13, 2000; Revised: October 10, 2001

Silicon carbide has been extensively used in structural applications, especially at high temperatures. In this work, Y_2O_3, Al_2O_3 and SiO_2 were added to β-SiC in order to obtain highly dense ceramics. Sintering was conducted in a dilatometer and in a graphite resistance furnace and the densification behaviour was studied. Sintered samples were characterised by density measurements, the crystalline phases were identified by X-ray diffraction. Microstructural observation of polished and polished/etched samples was carried out with help of scanning electron microscopy. Silicon carbide ceramics with more than 90% of the theoretical density were obtained by pressureless sintering if a suitable proportion of the additives is used.

Keywords: *silicon carbide, dilatometric studies, liquid phase sintering, additives*

1. Introduction

Silicon carbide is an important ceramic used in structural applications, such as automotive heat engines, cutting tools, heat exchange and mechanical seals. These applications are possible because of the unique properties of silicon carbide based materials, including high temperature strength and low density, as compared to conventional steel, and excellent thermal shock and wear resistance[1,2].

The chemical bonds between silicon and carbon atoms in SiC are almost 88% covalent, decreasing the atomic diffusivity and making it difficult to achieve high densification[3]. Sintering additives are usually required to obtain high density, such as boron, carbon, aluminium - or their compounds[4]. In these cases, sintering occurs through solid state mechanisms[5,6].

Liquid phase sintering, through solution re-precipitation process, can also be employed to densify SiC based ceramics[7-11]. The main advantage of this approach is the lower temperatures involved. Liquid phase is generally produced by reaction of the additives with SiO_2 present on the SiC surface[12-14].

Many parameters account for the production of highly dense ceramics, including powder properties such as high specific surface area, the processing technique used to consolidate the powders, and the sintering conditions, *i.e.* atmosphere, temperature and time. The control of sintering conditions is, therefore, of fundamental importance[15,16]. The amount and composition of the liquid phase can be formulated to provide suitable viscosity to make material transport more efficient and, consequently, to improve densification[17-19].

Sintering can be conducted in a dilatometer or in a graphite resistance furnace. Dilatometric measurements enable a study of sintering providing the temperatures of maximum shrinkage. Sintering in a dilatometer presents the disadvantage of greater weight loss and longer periods of time to reach equilibrium conditions. The latter is due to the continuous gas flow employed during experiments, which leads to variable pressure within the system. Sintering in graphite resistance furnace can be more effective due to the presence of a powder bed covering the samples, which helps maintain the vapour pressure constant and decrease the sample weight loss.

Sintering additives based on the SiO_2-Al_2O_3-Y_2O_3 system (another rare earth oxide may replace Y_2O_3) have been found to be suitable to promote SiC densification through liquid phase sintering[20-22]. These additives have also shown to be effective to obtain high density silicon nitride ceramics[23-25]. The formation of a eutectic temperature at about 1350 °C[26] is responsible for liquid formation that can dissolve the silicon carbide particles at relatively low temperatures. Pressureless sintering of silicon carbide is,

e-mail: jmarchi@net.ipen.br
Trabalho apresentado no 14° CBECIMAT, Águas de São Pedro, Dezembro de 2000.

therefore, possible using these additives, probably through a similar mechanism to that described for silicon nitride sintering. SiC grain morphology can be controlled by several processing conditions during sintering. In the present work, the sintering behaviour of silicon carbide using variable proportions of SiO_2-Al_2O_3-Y_2O_3 was investigated. The sintered samples were characterised in terms of densities, crystalline phases and microstructural observation. The influence of the oxides proportion on these parameters can be established.

2. Experimental

Powders of Y_2O_3 (H. C. Stark), SiO_2 (Sigma Aldrich) and Al_2O_3 (A16, Alcoa) were stirred for 4 h in several proportions, according to Table 1. The 60-20Y composition was also mixed using attritor mill (Szeguari) for 2 h.

Both processes, stirring and attrition milling, were tested in order to estimate the effects of the particle size distribution and mean particle size of the additives on the sintering behaviour of silicon carbide. For small amounts of additives, attrition mill is not usually recommended due to the high media wear during milling[27], although it provides better powder homogeneity.

All compositions of Table 1 were calculated without considering the low amount of SiO_2 (1.45%) which is present in SiC raw material. They are located schematically in the SiO_2-Al_2O_3-Y_2O_3 compositional diagram (Fig. 1). These compositions were chosen based on Shelby data[17], and are situated in the glass forming region. The 60-20Y mixture is located in the centre of this region. Thus, 90 vol % of β-SiC (BF 17, H. C. Stark) and 10 vol-% of each additive mixture were mixed and attritor milled for 4 h.

The theoretical densities of the additive mixtures, as well as of the final mixtures, were calculated using the mixture rule (Table 1). The particle size distribution of the raw material and mixtures was determined by the sedimentation technique (Sedigraph, 5100, 3.1). Particle morphology was observed using scanning electron microscopy (SEM).

The final mixtures were dried in a rotoevaporator (Heidolph WB 2000) and the powders were uniaxially pressed at 20 MPa. The samples were cold isostatically pressed at 200 MPa and the green densities determined.

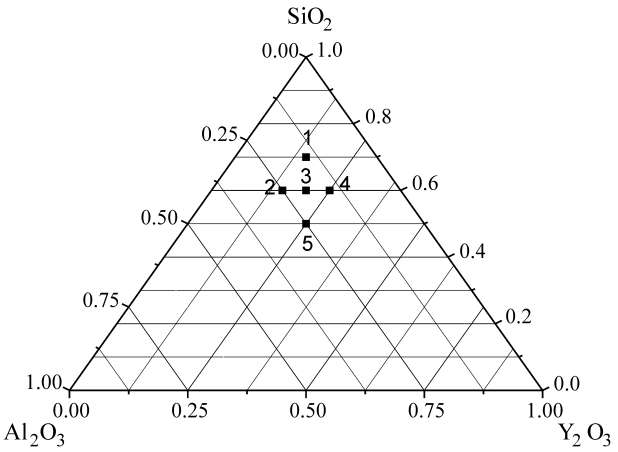

Figure 1. SiO_2-Al_2O_3-Y_2O_3 compositional diagram (mol %) with chosen data 1: 70-15Y; 2:60-15Y; 3: 60-20Y; 4:60-25Y; 5:50-25Y.

Sintering studies were performed in a dilatometer (Netzsch, DIL, 402 E/7), in either nitrogen or argon flow (1 atm), applying a heating rate of 15 °C/min up to 1950 °C. Samples were kept at this temperature for 1 h. The sintered samples were characterised for density using the geometrical and Archimedes methods.

In order to fully characterise the materials, the same compositions studied under dilatometry were pressureless sintered in a graphite resistance furnace, herein using protection powder bed of 60-20Y composition. The same schedule used in dilatometry experiments was applied, using only argon flow. Sintered samples were characterised for density and the samples were cut longitudinally. The crystalline phases of bulk samples were determined by X-ray diffraction (Phillips, PW, 1710). Microstructural observation was carried out using scanning electron microscope (Philips, XL, 30) on the longitudinal section of polished samples. These were prepared by traditional methods. The grain morphology was revealed after Murakami's etching. The etching solution was prepared by mixing KOH, $Fe_3K(CN)_6$ and distilled water in a ratio of 1:1:2.

3. Results and discussion

Table 1. Mixtures compositions, theoretical densities (% dt) and mean particle size (d50) of final mixtures.

Sample	% mol SiO_2	% mol Al_2O_3	% mol Y_2O_3	Y/A Ratio	% wt SiC	% wt additives	Theoretical densities		d50
							Additive	mixture	
60-20Y	60	20	20	1:1	88.68	11.32	3.2463	3.6630	0,44
50-25Y	50	25	25	1:1	88.18	11.82	3.2260	3.8603	0,42
70-15Y	70	15	15	1:1	89.32	10.64	3.2245	3.4449	0,44
60-25Y	60	15	25	5:3	88.47	11.53	3.2554	3.7538	0,42
60-15Y	60	25	15	3:5	88.99	11.01	3.2363	3.5643	0,45

3.1. Powder characterisation

Figure 2 depicts the particle size distribution of β-SiC and oxides used in this study, as well as of the 60-20Y composition after milling. The 60-20Y was chosen as a reference in the Fig. 2 to represent the typical behaviour of all other powder mixtures, which showed similar particle size distribution. The particle size distribution data provided the equivalent spherical diameter at a cumulative percentage of 50% (d50), as shown in Table 1. Figure 3 shows typical SEM observations of the additive mixture (60-20Y) and final mixture (additive and 90% volume of β-SiC). The powders are homogeneously mixed and do not contain large agglomerates. It is not possible to identify the different oxides through this technique. The mean particle size of the final powder mixture observed under SEM is in good agreement with the particle size distribution previously presented. Both techniques reveal the presence of a small fraction of particles larger than 1 μm.

3.2. Density

The densification results of 60-20Y samples, sintered in the dilatometer using either argon or nitrogen are shown in Fig. 4. This composition was prepared by mixing the additives in an attritor before milling with silicon carbide. Comparing the density after sintering (Table 2) and dilatometric curves (Fig. 4), one can see that the sample sintered under nitrogen does not undergo significant shrinkage. In this case, the nitrogen atoms are incorporated into the liquid, therefore increasing the liquid viscosity. This implies less wetting and the viscous liquid is not able to dissolve the silicon carbide particles. For this reason, further sintering experiments were conducted under argon atmosphere. These results agree with previously reported data[28] that compared

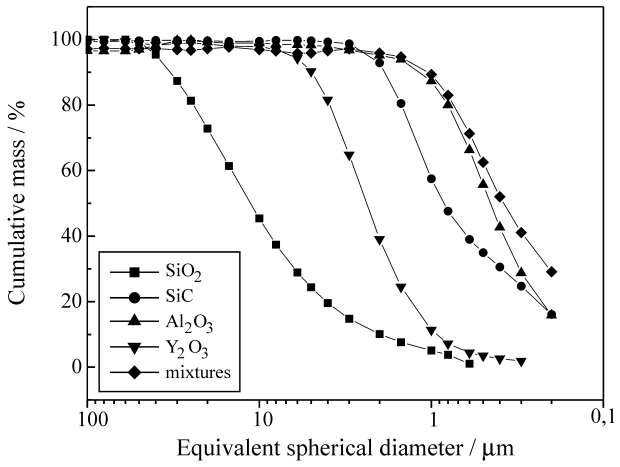

Figure 2. Particle/agglomerate size distribution of powder and a typical mixture (60-20Y).

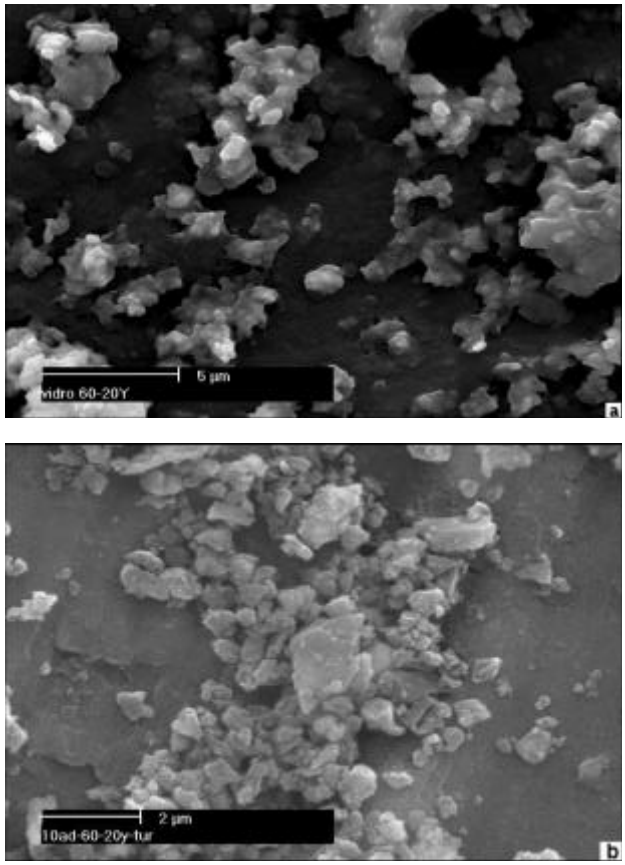

Figure 3. Powder scanning electron micrographs. a) typical additive mixture b) typical silicon carbide mixture (60-20Y).

both atmospheres and suggested argon flow as a more suitable atmosphere to obtain higher density.

<%-2>The sintered density data listed in Table 3 shows that samples sintered in the dilatometer exhibit lower density and higher weight loss when compared to samples sintered in the graphite resistance furnace. As previously mentioned, the samples sintered in the furnace were covered with a protective powder bed. This procedure has a marked influence on the results. Several samples of each composition were sintered under the same conditions, thus the results can be more representative than dilatometric samples.

The results obtained in the graphite furnace show that for higher weight loss the density decreases. Weigh loss occurs mainly due to additive volatilisation. Thus, weight loss could be minimised to achieve better densification.

Table 2. Sample 60-20Y densities (% theoretical) and weight loss (%) comparing the atmorphere.

Atmosphere	Green	Hidrostatic	Geometrical	Weight loss
nitrogen	54.7	64.3	63.3	10.2

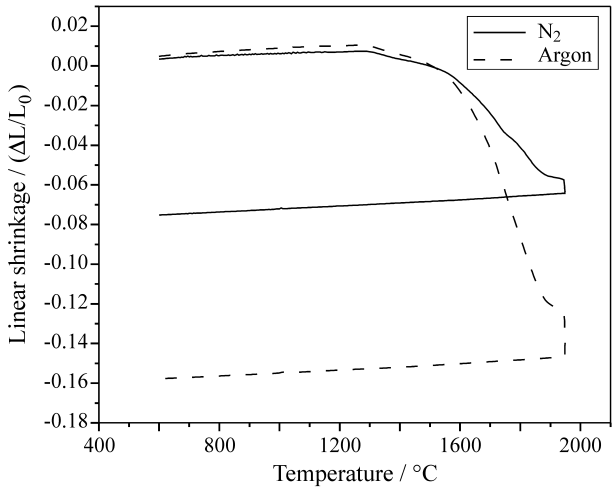

Figure 4. 60-20Y Dilatometric results: linear shrinkage versus temperature.

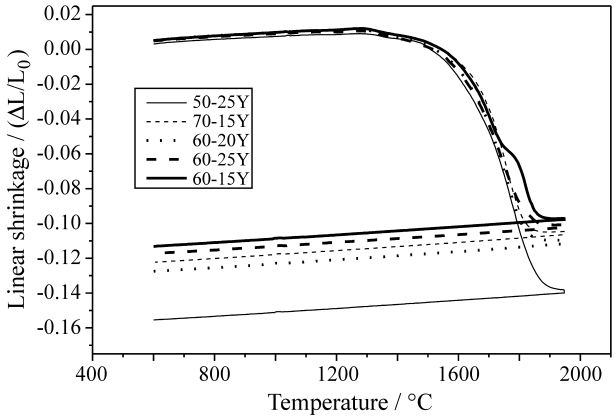

Figure 5. Dilatometric results in argon: linear shrinkage versus temperature for several compositions.

It is noted that keeping a constant Y_2O_3/Al_2O_3 ratio (1:1), while SiO_2 content is higher causes the density to decrease. When the SiO_2 amount is kept constant (60 mol%), the density increases as the Y_2O_3 amount is increased. This behaviour is probably related to the viscosity of the liquid formed, and depends on the solubility of silicon carbide. The literature points out the parameters that influence this mechanism[17,26], the most important being the viscosity and temperature of the liquid. The final density is related to the amount of liquid phase that could recrystallize. The final density of SiC compounds increases as the mixture density is higher. The best densities were obtained for the 50-25Y sample.

3.3. Dilatometric analysis

The density results obtained after sintering are in good agreement with the dilatometric curves presented in Fig. 5. The 50-25Y sample, which exhibits higher final density, shows higher shrinkage. It can be seen that at the temperature of 1950 °C there is no shrinkage, thus the densification process is hindered for all samples at such temperature.

The sintering behaviour of silicon carbide containing oxide additives is similar to that of silicon nitride based ceramics[23-25], implying that silicon carbide sintering occurs through liquid phase process.

The linear shrinkage rate (Fig. 6) reveals two shrinkage peaks. The first one, at lower temperature (at about 1300 °C) and broader, indicates a slight rearrangement of silicon carbide particles as the liquid phase starts to form, at a temperature near the eutectic. From the data of particle rearrangement shown in Table 4, one can see that the 60-20Y composition shows lower maximum shrinkage temperature. This temperature is related to the glass-forming region, and consequently, to the liquid composition formed during

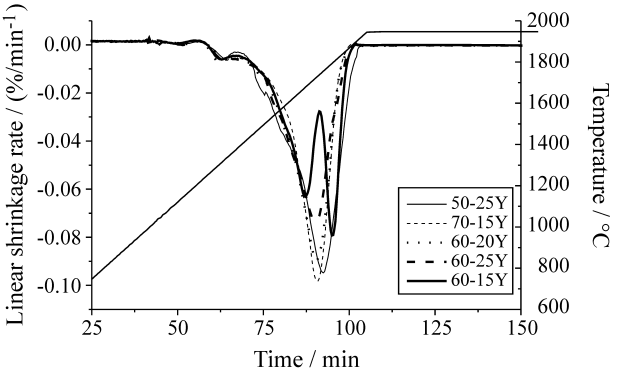

Figure 6. Dilatometric results: linear shrinkage rate versus time for several compositions.

Table 3. Samples densities (% theoretical) and weight loss (%) during sintering.

Sample	Dilatometer			Graphite furnance			
	green	hidrostatic	weight loss	green	hidrostatic	geometrical	weight loss
50-25Y	53.8	80.8	14.9	53.6 ∫ 0.1	91.9 ∫ 0.7	91.0 ∫ 0.5	7.6 ∫ 0.1
70-15Y	54.6	71.0	15.8	54.1 ∫ 0.1	86.2 ∫ 0.1	85.5 ∫ 0.4	9.3 ∫ 0.1
60-20Y	54.0	72.7	15.6	53.6 ∫ 0.1	89.2 ∫ 0.2	88.9 ∫ 0.3	8.3 ∫ 0.1
60-15Y	54.4	71.5	15.5	53.9 ∫ 0.1	86.9 ∫ 0.3	84.9 ∫ 0.4	9.2 ∫ 0.1
60-25Y	54.2	79.9	14.3	53.9 ∫ 0.2	89.8 ∫ 0.8	87.9 ∫ 0.1	7.8 ∫ 0.5

Table 4. Temperatures of maximum shrinkage due to particle rearrangement (Tr) and due to solution reprecipitation (Tsr).

Sample	Tr	Trs
50-25Y	1325	1755
70-15Y	1320	1730
60-20Y	1300	1725
60-15Y	1315	1680 and 1795 *
60-25Y	1310	1725

*: two maximum temperatures due to solution reprecipitation.

the first sintering stage. The maximum rearrangement temperature seems to be lower as the centre of the glass-forming region is approached, even though it does not lead to improve densification.

The sharper peak observed at higher temperature in Fig. 6 represents the formation of larger quantities of liquid and simultaneous dissolution of silicon carbide particles (solution-reprecipitation process). Exception to this is noted for 60-15Y composition.

The maximum shrinkage temperature data for liquid formation and solution-reprecipitation process is given in Table 4. The 50-25Y sample has higher density and shows higher maximum shrinkage temperature. The other samples show similar maximum shrinkage temperature, but different final density, suggesting that other parameters are involved in the densification process.

Simultaneous liquid formation and solution-reprecipitation process is not observed for 60-15Y sample. This sample shows two distinct maximum shrinkage at higher temperatures, indicating that liquid formation and solution reprecipitation processes do not occur simultaneously. This observation should be investigated using compositional data; further studies are required to explain this

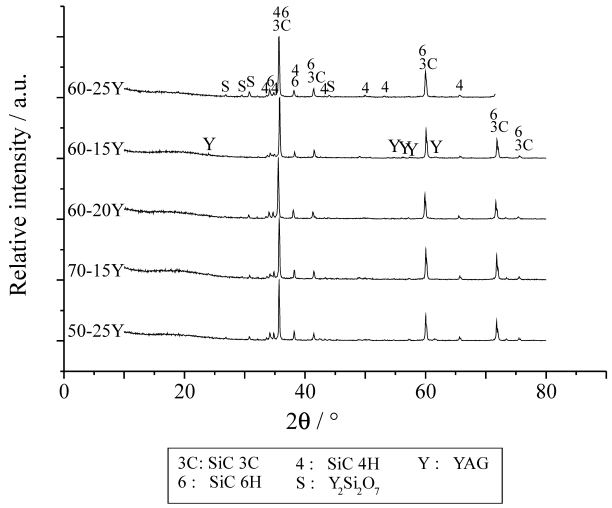

Figure 7. X-ray diffratograms of sintered samples.

behaviour. The densification process can be related, therefore, to the large amount of liquid that is determined by the *liquidus* temperature in the phase diagrams of SiO_2-Al_2O_3-Y_2O_3 system, which determines the liquid viscosity and the dissolution rate of silicon carbide particles.

3.4. Microstructural observation

The X-ray diffraction patterns of bulk samples are shown in Fig. 7. Three silicon carbide polytypes are present: 3C, 4H and 6H. The presence of the 3C polytype indicates that the β-α transformation is not complete. The phase $Y_2Si_2O_7$ was identified by X-ray diffraction as a crystalline secondary phase present in all samples. YAG ($Al_5Y_3O_{12}$) was also identified in the 60-15Y composition, keeping constant the ratio 3 Y_2O_3: 5 Al_2O_3 as well as the initial additive content. The presence of this phase could be related to the two maximum shrinkage peaks observed in dilatometry for the same sample. It is possible that YAG is also formed in the other compositions, but only in small quantities, which are not detectable by X-ray diffraction analysis.

Figure 8a shows a typical micrograph of a polished surface observed under scanning electron microscopy. The secondary phase appears to be well distributed in all samples,

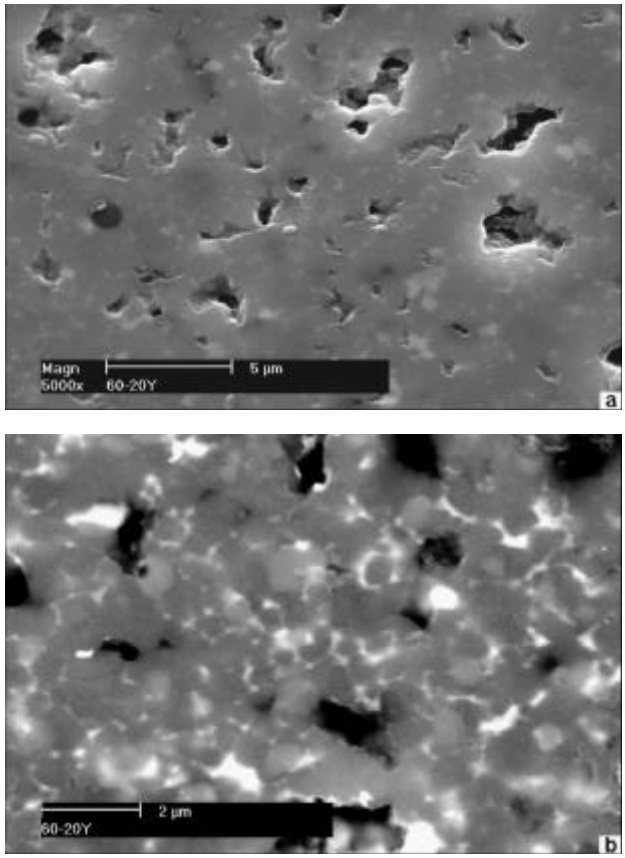

Figure 8. Typical scanning electron micrograph of sintered sample. a) after polishing; b) after Murakami's etching.

indicating good mixture homogeneity. The micrographs of etched samples reveal the morphology of silicon carbide grains (Fig. 8b). All sintered samples have similar microstructure without secondary grain growth.

4. Conclusions

The use of 90% β-SiC, with several proportions of SiO_2, Y_2O_3 and Al_2O_3 as additives, was suitable to obtain silicon carbide with about 90% density by pressureless sintering.

Dilatometric experiments revealed the presence of two shrinkage peaks during sintering of silicon carbide. The first is related to a slight particle rearrangement and a second peak, at higher temperatures, indicates liquid formation and solution re-precipitation.

The samples sintered in the presence of powder bed in a graphite resistance furnace show a lower weight loss and, therefore, higher densification. X-ray diffraction revealed the presence of β-SiC (3C polytype) and α-SiC (4H and 6H polytype) as well as small amounts of $Y_2Si_2O_7$ and YAG.

Acknowledgements

The authors thank CNPq, PRONEX and FAPESP for financial support. The technical discussions with colleagues of the Department of Ceramics - IPEN are fully appreciated.

References

1. Somiya, S.; Inomata, Y. Silicon Carbide Ceramics, Ed. Elsevier Applied Science, 1991.
2. Panpuch, R. *J. Euro. Ceram. Soc.*, v. 18., p. 993-1000, 1998.
3. Frevel, L.K.; Petersen, D.R.; Saha, C.K. *J. Mater. Sci.*, v. 27, p. 1913-1925, 1992.
4. Negita, K. *J. Am. Ceram. Soc.*, v. 69, p. c308-c310, 1986.
5. Rifskijk, W.V.; Shanefield, D.J. *J. Am. Ceram. Soc.*, v. 73, p. 148-149, 1990.
6. Prochazka, S. *British Ceram. Res.*, p. 171-181, 1975.
7. Keppeler, M.; Reichert, H.G.; Broadley, J.M.; Thurn, G.; Wiedmann, I.; Aldinger, F. *J. Euro. Ceram. Soc.*, v. 18, p. 521-526, 1998.
8. Pan, Y.; Baptista, J.L. *J. Euro. Ceram. Soc.*, v. 16, p. 1221-1230, 1996.
9. Dijen, F.K.V.; Mayer, E. *J. Euro. Ceram. Soc.*, v. 16, p. 413-420, 1996.
10. Grande, T.; Sommerset, H.; Hagen, E.; Wiik, K.; Einarsrud, M.A. *J. Am. Ceram. Soc.*, v. 80, p. 1047-1052, 1997.
11. Strecker, K.; Ribeiro, S.; Camargo, D.; Silva, R.; Vieira, J.; Oliveira, F. *Mat. Res.*, v. 2, p. 249-254, 1999.
12. Izhevskyi, V.A.; Genova, L.A.; Bressiani, A.H.A.; Bressiani, J.C. Proceedings of 7th International Symposium Ceramic Materials and Components for Engines - Germany, June, 19-21, 2000.
13. Marchi, J.; Bressiani, J.C.; Bressiani, A.H.A. *Key Eng. Mater.*, v. 189-191, p. 120-125, 2001.
14. Lee, J.K.; Tanaka, H.; Kim, H.; Kim, D.J. *Mater. Letters*, v. 29, p. 135-142, 1996.
15. She, J.; Jiang, D.; Tan, S.; Guo, J. *Mater. Letters*, v. 14, p. 240-244, 1992.
16. Shinozaki, S.S.; Hangas, J.; Carduner, K.R.; Rokosz, M.J.; Suzuki, K., Shinohara, N. *J. Mater. Res.*, v. 8, p. 1635-1643, 1993.
17. Shelby, J.E. *Key Eng. Mat.*, v. 94-95 p. 181-208, 1994.
18. Shelby, J.E.; Kohli, J.T. *J. Am. Ceram. Soc.*, v. 73, p. 39-42, 1990.
19. Sun, W.Y.; Tu, H.Y.; Wang, P.L.; Yan, D.S. *J. Euro. Ceram. Soc.*, v. 17, p. 789-196, 1997.
20. Chen, Z. *Mater. Letters*, v. 17, p. 27-80, 1993.
21. Omori, M.; Takei, H. *J. Mater. Sci.*, v. 23, p. 3744-3749, 1988.
22. Mulla, M.A.; Krstic, V.D. *Am. Ceram. Soc. Bull.*, v. 70, p.439-443, 1991.
23. Camusai, N.; Thompson, D.P.; Mandal, H. *J. Euro. Ceram. Soc.*, v. 17, p. 599-613, 1997.
24. Hirosaki, N.; Okada, A.; Matoba, K. *J. Am. Ceram. Soc.*, v. 71, p. c144-c147, 1988.
25. Huang, Z.K.; Rosenflanz, A.; Chen, I.W. *J.Am. Ceram. Soc.*, v. 80, p. 1256-1262, 1997
26. Kolitsch, U.; Seifert, H.J.; Aldinger, F. *J. Phase Eq.*, v. 19, p. 426-433, 1998
27. Padden, S.A.; Reed, J.S. *Am. Ceram. Soc. Bull.*, v. 72, p. 101, 1993
28. De Carvalho, M.T.; da Silva, O.M.M.; Strecker, K.; da Silva, C.R.M. *Key Eng. Mater.*, v. 189-191, p. 126-131, 2001.

FAPESP helped in meeting the publication costs of this article